# Deficiency or Mutation of Presenilin Genes Lead to the Dysregulation of Amino Acid Sensing by mTORC1

Kavya Reddy[1], Corey L. Cusack[1], Israel C. Nnah[1], Khoosheh Khayati[1], Chaitali Saqcena[1], Tuong B. Huynh[2,3], Scott A. Noggle[4], Andrea Ballabio[2,3,5,6] and Radek Dobrowolski[1]

[1]Glenn Biggs Insitute for Alzheimer's and Neurodegenerative Diseases, San Antonio, TX, USA. [2]Department of Molecular and Human Genetics, Baylor College of Medicine, Houston, USA. [3] Jan and Dan Duncan Neurological Research Institute, Texas Children Hospital, Houston, USA.
[4] The New York Stem Cell Foundation Research Institute, New York, NY 10032, USA[5] Telethon Institute of Genetics and Medicine (TIGEM), Pozzuoli, Naples, Italy. [6] Medical Genetics, Department of Translational Medicine, Federico II University, Naples, Italy

SUMMARY

Attenuated auto-lysosomal system has been associated with Alzheimer's disease (AD), yet the underlying molecular mechanisms leading to this impairment are largely unknown. We show that the amino acid sensing of mechanistic target of Rapamycin complex 1 (mTORC1) is dysregulated in cells deficient in Presenilin, a protein associated with AD. In these cells, mTORC1 is constitutively tethered to lysosomal membranes, unresponsive to starvation, and inhibitory to TFEB-mediated clearance due to a reduction in Sestrin 2 expression. Normalization of Sestrin 2 levels through overexpression or elevation of nuclear calcium rescued mTORC1 tethering and initiated clearance. While CLEAR network attenuation in vivo results in buildup of amyloid, phospho-Tau, and neurodegeneration, Presenilin-KO fibroblasts and iPSC-derived AD human neurons fail to effectively initiate autophagy and degenerate in long-term starvation assays. These results propose an altered mechanism for nutrient sensing in presenilin deficiency and underline the importance of clearance pathways in the onset of AD.
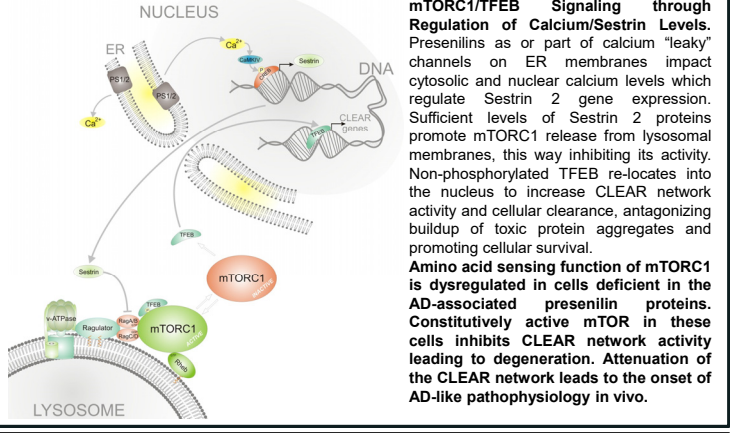
Figure 1: **Model of Presenilin Function in mTORC1/TFEB Signaling through Regulation of Calcium/Sestrin Levels.** Presenilins as or part of calcium "leaky" channels on ER membranes impact cytosolic and nuclear calcium levels which regulate Sestrin 2 gene expression. Sufficient levels of Sestrin 2 proteins promote mTORC1 release from lysosomal membranes, this way inhibiting its activity. Non-phosphorylated TFEB re-locates into the nucleus to increase CLEAR network activity and cellular clearance, antagonizing buildup of toxic protein aggregates and promoting cellular survival.

Amino acid sensing function of mTORC1 is dysregulated in cells deficient in the AD-associated presenilin proteins. Constitutively active mTOR in these cells inhibits CLEAR network activity leading to degeneration. Attenuation of the CLEAR network leads to the onset of AD-like pathophysiology in vivo.


RESULTS
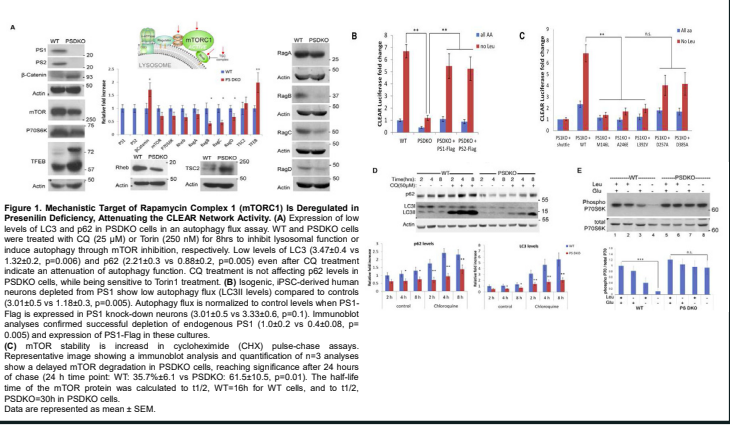
Figure 1. Mechanistic Target of Rapamycin Complex 1 (mTORC1) Is Deregulated in Presenilin Deficiency, Attenuating the CLEAR Network Activity. (A) Expression of low levels of LC3 and p62 in PSDKO cells. In autophagy flux assay, WT and PSDKO cells were treated with CQ (25 μM) or Torin (250 nM) for 8hrs to inhibit lysosomal function or induce autophagy through mTOR inhibition, respectively. Low levels of LC3 (3.47±0.4 vs 1.32±0.2, p=0.006) and p62 (2.21±0.3 vs 0.88±0.2, p=0.005) even after CQ treatment indicate an attenuation of autophagic function. CQ treatment is not affecting p62 levels in PSDKO cells, while being sensitive to Torin1 treatment. **(B)** Isogenic, iPSC-derived human neurons depleted from PS1 show low autophagy flux (LC3II levels) compared to controls (3.01±0.5 vs 1.18±0.3, p=0.0005). Autophagy flux is normalized to control levels in PS1 knock-down neurons (1.0±0.2 vs 3.33±0.6, p=0.1). Immunoblot analyses confirmed successful depletion of endogenous PS1 (PS1-Flag) in these cultures.
(C) mTOR stability is increased in cycloheximide (CHX) pulse-chase assays. Representative image showing a immunoblot analysis and quantification of n=3 analyses show a delayed mTOR degradation in PSDKO cells, reaching significance after 24 hours of chase (24 h time point: WT: 35.7%±6.1 vs PSDKO: 61.5±10.5, p=0.01). The half-life time of the mTOR protein was calculated to t1/2, WT=16h for WT cells, and to t1/2, PSDKO=30h in PSDKO cells.
Data are represented as mean ± SEM.
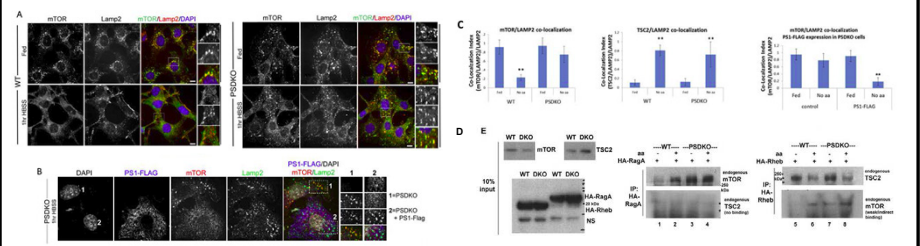
Figure 2. Defective amino acid sensing of mTORC1 in PSDKO Cells is Mediated by Excessive RagA binding And Independent of TSC2 Localization. (A) mTOR re-localizes back to LAMP2 vesicles at 4hrs of starvation, and is found on lysosomes at the same time in TSC2. WT cells were starved for 1hr, 2hr and 4hr in HBSS and the localization of mTOR/TSC2 and Lamp2 was determined by immunostaining. Quantification of lysosomal co-localization: at 1 h time point: mTOR 0.76±0.2 vs TSC2: 0.8±0.3. (B) (B) TSC2 localization upon starvation and re-feeding is normal in PSDKO cells. WT and PSDKO cells were starved for 1hr in HBSS and re-fed with nutrient rich media. Insets depict selected fields that were magnified. Quantification of lysosomal co-localization, 1 h after starvation WT: 0.79±0.1 vs PSDKO: 0.8±0.2, 1h after aa re-feeding WT 0.1±0.04 vs PSDKO 0.12±0.01.
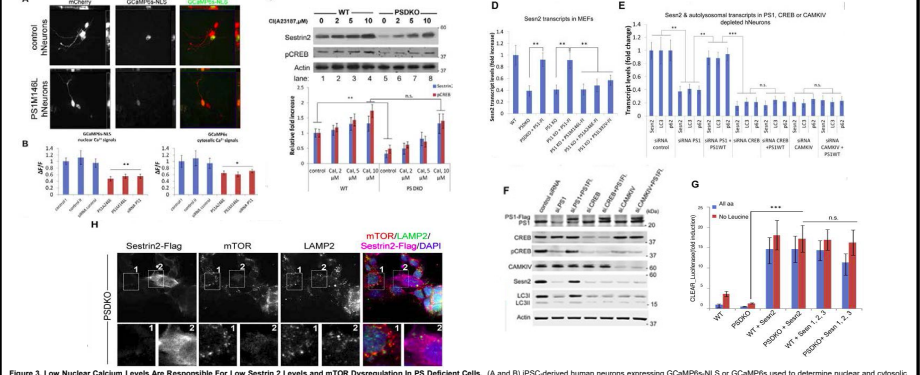
Figure 3. Low Nuclear Calcium Levels Are Responsible For Low Sestrin 2 Levels and mTOR Dysregulation In PS Deficient Cells. (A and B) iPSC-derived human neurons expressing GCaMP6s-NLS or GCaMP6s used to determine nuclear and cytosolic calcium levels. mCherry was used to visualize neuronal projections which are largely excluded when GCaMP6s-NLS vectors were used. Images show orthogonal maximal intensity projections of x/y, x/z, and y/z perspectives.PS1M146L, PS1A246E and PS1 siRNA depleted mutant neurons show a significant reduction of cytosolic and more significant nuclear calcium levels (for cytosolic calcium levels: PS1M146L: 0.7±0.05, p=0.05; for nuclear calcium levels: PS1M146L 0.55±0.06, and PS1A246E 0.48±0.07, siRNA PS1: 0.52±0.06, p=0.01). (C) Elevated cellular calcium increases the otherwise low Sestrin2 levels in PSDKO cells. WT and PSDKO cells were treated with increasing concentrations of Calcium Ionophore (CI, 2 μM to10 μM) overnight followed by analyses for pCREB and Sestrin 2 protein levels (baseline pCREB levels: WT 1±0.14 vs PSDKO 0.47±0.11, p=0.01; pCREB after Cal, 10μM: WT 1.7±0.2 vs PSDKO 0.89±0.3, p=0.1, baseline Sesn2 levels: WT 1±0.1 vs PSDKO 0.3±0.1, p=0.01; Sesn2 after Cal, 10μM: WT 1.3±0.3 vs PSDKO 1.3±0.2, p=0.01). (D) PS regulates Sestrin 2 transcription. Sesn2 transcript levels are low in PS knock-out cells an increase with expression of exogenous PS1WT-Flag constructs, while AD-associated PS mutations do not (PSDKO+PS1-Flag: 0.92±0.1 and PS1KO+PS1-Flag: 0.91±0.1 vs PS1M146L: 0.41±0.1, A246E: 0.48±0.2 L392V: 0.6±0.1 p=0.01). (E and F) Sestrin 2 expression is dependent on PS1, CREB and CaMKIV. qPCR analysis in (E) show low Sesn2, LC3 and p62 mRNA levels when PS1, CREB or CaMKIV are depleted in human neuronal cultures (for Sesn2 levels: siRNA control: 1±0.1 vs siRNA PS1: 0.37±0.1, siRNA CREB: 0.2±0.1, and siRNA CaMKIV: 0.2±0.1, p=0.001). Expression of exogenous PS1WT-Flag rescues LC3, p62 and Sesn2 levels only in PS1 depleted neurons (0.89±0.1, p=0.1 to control). Immunoblot analyses in (F) show the expression of the samples on protein level, all used siRNA pools depleted protein levels to at least 40% of their control levels. (G) Overexpression of Sestrin1, 2, 3 or Sestrin 2 alone rescues the attenuated CLEAR induction in PSDKO cells in CLEAR-luciferase reporter assays (1.35±0.15 vs 17.3±3.3, p=0.001, left bracket). (H) Overexpression of Sestrin-Flag in PSDKO cells disperses the otherwise tethered mTORC1 to lysosomes. PSDKO cells is labeled with "1", Sestrin2-Flag expressing cell is depicted as "2". mTOR diffusion is visible in single channel images of cell #2 (PSDKO: 0.88±0.3 vs PSDKO+Sesn2-Flag: 0.26±0.1, n=200, p=0.05). Data are represented as mean ± SEM.
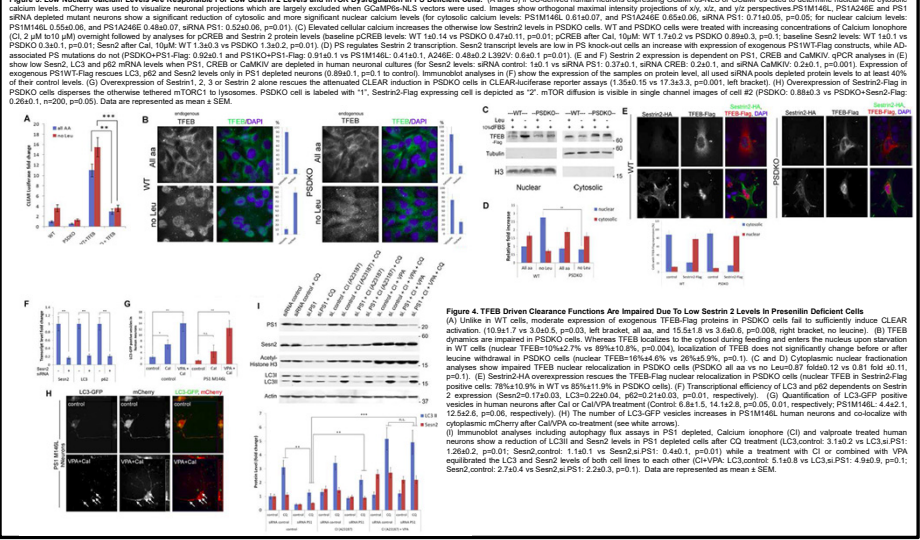
Figure 4. TFEB Driven Clearance Functions Are Impaired Due To Low Sestrin 2 Levels In Presenilin Deficient Cells (A) Unlike in WT cells, moderate expression of exogenous TFEB-Flag proteins in PSDKO cells fail to sufficiently induce CLEAR activation. (10.9±1.7 vs 3.5±0, p=0.03, left bracket, all aa, and 15.5±1.8 vs 3.6±0.6, p=0.008, right bracket, no leucine). (B) TFEB dynamics are impaired in PSDKO cells. Whereas TFEB localizes to the cytosol during feeding and enters the nucleus upon starvation in WT cells (nuclear TFEB=10%±2.7% vs 89%±10.8%, p=0.004), localization of TFEB does not significantly change before or after leucine withdrawal in PSDKO cells (nuclear TFEB=16%±4.6% vs 26%±5.9%, p=0.1). (C and D) Cytoplasmic nuclear fractionation analyses show impaired TFEB nuclear relocalization in PSDKO cells (nuclear TFEB-Flag positive cells: 78%±10.9% in WT vs 85%±11.9% in PSDKO cells). (F) Transcriptional efficiency of LC3 and p62 depends on Sestrin 2 expression (Sesn2=0.17±0.03, LC3=0.22±0.04, p62=0.21±0.03, p=0.01, respectively). (G) Quantification of LC3-GFP positive vesicles in human neurons after Cal or Cal/VPA treatment (Control 6.8±1.5, 14.1±2.8, p=0.05, 0.01, respectively; PS1M146L: 4.4±2.1, 12.5±2.6, p=0.06, respectively). (H) Number of LC3-GFP vesicles increases in PS1M146L human neurons in PS1 depleted, Calcium ionophore (CI) and valproate treated human neurons show a reduction of LC3 and Sesn2 levels in PS1 depleted cells after CQ treatment (LC3,control: 3.1±0.2 vs LC3,siPS1: 1.26±0.2, p=0.01; Sesn2,control: 1.1±0.1 vs Sesn2,si.PS1: 0.4±0.1, p=0.01) while a combined with CI or combined with VPA equilibrated the LC3 and Sesn2 levels of both cell lines to each other (CI+VPA: LC3,control: 5.1±0.8 vs LC3,si.PS1: 4.9±0.9, p=0.1; Sesn2,control: 2.7±0.4 vs Sesn2,si.PS1: 2.2±0.3, p=0.1). Data are represented as mean ± SEM.
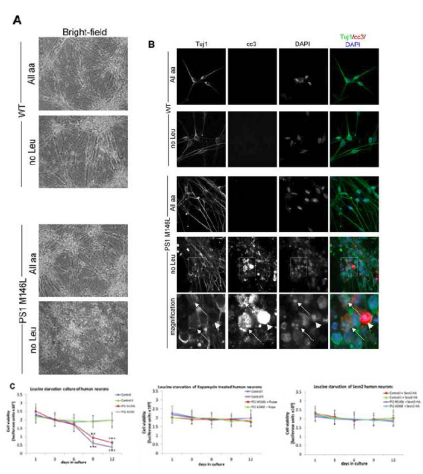
Figure 5. Presenilin Deficient Human Neurons Degenerate in Long-Term Leucine Starvation Assays.
(A) Control (WT) or FAD (PS1M146L or PS1A246E) human neurons were cultured in media containing either all amino acids (All aa) or lacking leucine (no Leu). Degeneration of FAD (PS1M146L shown here) neurons is evident in bright-field microscopy when starved from leucine.
(B) Immunofluorescence analyses of same cultures as in (A) indicate a buildup of cleaved caspase 3 (cc3) and fragmented nuclei in leucine starved FAD (PS1M146L shown here) neurons (64%±7.6% of all cells, p=0.005). Arrows depict cells with nuclear cc3 and pyknotic nuclei, arrow head points to soma with highly accumulated cc3 in magnified region.
(C) Biochemical viability assays show a significant reduction of ATP levels in PS1M146L or PS1A246E before the 9th day of leucine starvation. Rapamycin treatment (middle panel) or expression of exogenous Sestrin2-HA in same neuronal cultures inhibited their degeneration.
(D) Autophagy flux assays show an attenuation of LC3-II levels in baseline or after Chloroquine (CQ) treatment in FAD neurons in comparison to both control lines (FAD baseline: M146L: 0.33±0.05, A246E: 0.36±0.05 after CQ: 0.89±0.1, 1.43±0.2, respectively, p=0.01), while Sestrin2 levels were reduced (M146L: 0.38±0.06, A246E: 0.51±0.1, p=0.01) and the ratio between p-ULK1/total ULK1 was increased in the baseline and after CQ treatment (M146L and A246E, respectively at baseline: 2.67±0.3, 3.11±0.4, p=0.01 and after CQ: 2.21±0.25, 2.11±0.3, p=0.001).
(E) Expression of exogenous Sestrin2 (-HA) inhibits mTORC1 activity, TFEB phosphorylation and restores autophagy levels in FAD human neurons. High mTORC1 activity (M146L: 2.87±0.5, A246E: 2.91±0.4, p=0.01 to controls), TFEB phosphorylation (M146L: 2.4±0.6, A246E: 2.71±0.4, p=0.01 to controls), and low LC3II levels (M146L: 0.3±0.04, A246E: 0.4±0.05, p=0.01 to controls) are present in neurons carrying the PS1 FAD mutations, while overexpression of Sestrin2-HA rescues FAD cells by elevating LC3 levels (M146L: 1.88±0.3, A246E: 1.79±0.2, p=0.01) and reducing mTORC1 activity (M146L: 0.43±0.06, A246E: 0.4±0.06, p=0.01 to baseline FAD).
Data are represented as mean ± SEM.

REFERENCES

- Bading, H. (2013). Nuclear calcium signalling in the regulation of brain function. Nat. Rev. Neurosci. 14, 593–608.
- Bhojak, T.J., DeKosky, S.T., Ganguli, M., and Kamboh, M.I. (2001). Genetic polymorphism in the cathepsin G gene and the risk of Alzheimer's disease. Neurosci. Lett. 309, 138–140.
- Cataldo, A.M., Barnett, J.L., Pieroni, C., and Nixon, R.A. (1997). Increased neuronal endocytosis and protease delivery to early endosomes in sporadic Alzheimer's disease: neuropathologic evidence for a mechanism of increased beta-amyloidogenesis. J. Neurosci. 17, 6142–6151.
- Chambers, S.M., Fasano, C. a, Papapetrou, E.P., Tomishima, M., Sadelain, M., and Studer, L. (2009). Highly efficient neural conversion of human ES and iPS cells by dual inhibition of SMAD signaling. Nat. Biotechnol. 27, 275–280.
- Chantranupong, L., Wolfson, R.L., Orozco, J.M., Saxton, R.A., Scaria, S.M., Bar-Peled, L., Spooner, E., Isasa, M., Gygi, S.P., and Sabatini, D.M. (2014). The Sestrins Interact with GATOR2 to Negatively Regulate the Amino-Acid-Sensing Pathway Upstream of mTORC1. Cell Rep. 9, 1–8.
- McBrayer, M., and Nixon, R.A. (2013). Lysosome and calcium dysregulation in Alzheimer's disease: partners in crime. Biochem. Soc. Trans. 41, 1495–1502.
- Medina, D.L., Di Paola, S., Peluso, I., Armani, A., De Stefani, D., Venditti, R., Montefusco, S., Scotto-Rosato, A., Prezioso, C., Forrester, A., et al. (2015). Lysosomal calcium signalling regulates autophagy through calcineurin and TFEB. Nat. Cell Biol. 17, 288–299.
- Megahara, A., Ravel, A., Mircher, C., Sturtz, F., Grattau, Y., Rethoré, M.-O., Delabar, J.-M., and Mobley, W.C. (2009). The 50th anniversary of the discovery of trisomy 21: the past, present, and future of research and treatment of Down syndrome. Genet. Med. 11, 611–616.
- Menon, S., Dibble, C.C., Talbott, G., Hoxhaj, G., Valvezan, A.J., Takahashi, H., Cantley, L.C., and Manning B.D. (2014). Spatial control of the TSC complex integrates insulin and nutrient regulation of mTORC1 at the lysosome. Cell 156, 771–785.
- Mi, W., Pawlik, M., Sastre, M., Jung, S.S., Radinsky, D.S., Klein, A.M., Sommer, J., Schmidt, S.D., Nixon, R.A., Mathews, P.M., et al. (2007). Cystatin C inhibits amyloid-beta deposition in Alzheimer's disease mouse models. Nat. Genet. 39, 1440–1442.
- Nixon, R. (2013). The role of autophagy in neurodegenerative disease. Nat. Med. 19, 983–997.
- Nixon, R.A., and Yang, D.S. (2011). Autophagy failure in Alzheimer's disease—locating the primary defect. Neurobiol. Dis. 43, 38–45.
- Nixon, R.A., Wegiel, J., Kumar, A., Yu, W.H., Peterhoff, C., Cataldo, A., and Cuervo, A.M. (2005). Extensive involvement of autophagy in Alzheimer disease: an immuno-electron microscopy study. J. Neuropathol. Exp. Neurol. 64, 113–122.
- Nnah, I.C., Khayati, K., and Dobrowolski, R. (2015) Cellular Metabolism and Lysosomal mTOR signaling. Cell Death Ther. 1.

RESULTS